Low Temperature Physics/Fizika Nizkikh Temperatur, 2016, v. 42, No. 6, pp. 573–580

Cascade of parametric resonances in coupled Josephson junctions

Yu.M. Shukrinov[1,2], H. Azemtsa-Donfack[3], I.R. Rahmonov[1,4], and A.E. Botha[3]

[1]*BLTP, JINR, Dubna, Moscow Region 141980, Russia*
E-mail: shukrinv@theor.jinr.ru
yurishukrinov@yahoo.com

[2]*Dubna University, Dubna, Moscow Region 141980, Russia*

[3]*Department of Physics, University of South Africa, Science Campus, Private Bag X6, Florida 1710, South Africa*

[4]*Umarov Physical Technical Institute, TAS, Dushanbe 734063, Tajikistan*

Received March 9, 2016, published online April 25, 2016

We found that the coupled system of Josephson junctions under external electromagnetic radiation demonstrates a cascade of parametric instabilities. These instabilities appear along the *IV* characteristics within bias current intervals corresponding to Shapiro step subharmonics and lead to charging in the superconducting layers. The amplitudes of the charge oscillations increase with increasing external radiation power. We demonstrate the existence of longitudinal plasma waves at the corresponding bias current values. An essential advantage of the parametric instabilities in the case of subharmonics is the lower amplitude of radiation that is needed for the creation of the longitudinal plasma wave. This fact gives a unique possibility to create and control longitudinal plasma waves in layered superconductors. We propose a novel experiment for studying parametric instabilities and the charging of superconducting layers based on the simultaneous variation of the bias current and radiation amplitude.

PACS: 85.25.Cp Josephson devices;
74.50.+r Tunneling phenomena; Josephson effects;
74.20.–z Theories and models of superconducting state;
05.45.–a Nonlinear dynamics and chaos.

Keywords: Josephson effect, tunneling, chaos, Shapiro step subharmonics.

1. Introduction

Coupled Josephson junctions (JJs) are used to model the intrinsic junctions in layered superconductors, which found important applications in superconducting electronics and generation of electromagnetic waves in terahertz frequency region [1]. For this reason the properties of the models based on coupled JJs continue to attract much attention. Specific features of the coupling between junctions are related to the generalized Josephson relation [2,3] and the creation of a longitudinal plasma wave along the stack [4].

JJs under external electromagnetic radiation possess important features which are used in a variety of applications [5,6]. In the quantum voltage standard, thousands of junctions in series are required to obtain Shapiro steps at sufficiently high voltages [7]. The intrinsic JJs in high-temperature superconductors offer a possibility to realize a large number of junctions in a very compact way [8–10]. Compared to the well-developed low-T_c voltage standards, a few advantages can be found using intrinsic JJs; like, high operation temperatures, operation at higher frequencies (up to THz) and high density of junctions due to the naturally more compact atomic scale, which may simplify the instrumentation significantly [9,11].

A stack of coupled JJs shows more complex physics in comparison to the case of a single junction [1,8,12]. The external radiation leads additionally to a series of novel effects related to the coupling between junctions, parametric instabilities and the excitation of a longitudinal plasma wave (LPW) propagating along the c axis of the stack [4,13,14]. As it is well known, the frequency-locking of the Josephson oscillations with frequency ω_J to the frequency ω of external electromagnetic radiation leads to the appearance of Shapiro steps (SS) and their subharmonics in

the current–voltage characteristics (*IV* characteristics) [15]. Many devices in existence, based on the traditional superconductors, exploit this effect [5], notably voltage standards and terahertz radiation emitters/detectors [1]. Therefore, a detailed study of the SS and SS subharmonics in the intrinsic JJs under different resonance conditions presents important research questions with various potential applications. The appearance of charge in the superconducting layers (S layers) in the current interval corresponding to the SS harmonics was studied in Ref. 14. However, the peculiarities of charging of the S layers in the current interval corresponding to the SS subharmonics have not been studied yet.

In this paper we discuss results related to the effects of electromagnetic radiation on the phase dynamics of the intrinsic JJs and the temporal oscillations of the electric charge in the S layers. For fixed parameters of JJs, we demonstrate the "charging" of the Shapiro step subharmonics in the *IV* characteristics, i.e., the charging of S layers in the corresponding bias current intervals at different amplitudes of external radiation. To escape the complexity related to the overlapping of the SS subharmonics, we use radiation with small amplitudes. We have found an essential difference between the parametric instabilities in case of subharmonics and Shapiro steps: in the case of subharmonics a much lower amplitude of radiation is needed for the creation of the longitudinal plasma waves along the stack. This fact provides a unique possibility to create and control these waves in layered superconductors and might be important for future applications. We describe the physics of this phenomena and show how a charge appears in S layers with increasing amplitude of the external radiation. The variation of the amplitude of external electromagnetic radiation changes the wavelength of the LPW [14]. This sensitivity to the external radiation might play an important role for the synchronization of Josephson oscillations in the stack [16]. A clear understanding of this phenomenon could potentially provide a new way for experimentalists to try an increasing the power of the emitted electromagnetic radiation in the terahertz region. However, there are still many open questions concerning the excitation of the LPW. Particularly, the possibility of exciting the LPW at lower power of external radiation. Here we demonstrate that the use of SS subharmonics may be one way of realizing this possibility.

The paper is organized in the following way. In Sec. 2, we introduce the coupled system of equations that is used in our numerical simulations. The numerical procedure is described briefly. In Sec. 3, we present the results of simulation, analysis of the *IV* characteristics at two different amplitudes and demonstrate general features of subharmonics appearance with increase in power of radiation. The charging of S layers is discussed in Sec. 4. We present a plot of the magnitude of the differential resistance as a function of the radiation amplitude and bias current and stress its importance. In Sec. 5, we prove the occurrence of the parametric instabilities within the current intervals corresponding to Shapiro step subharmonics. Finally, we discuss the obtained results and come to the conclusions.

2. Model and methods

For our numerical calculations we use the well-known methods described, for example, in Refs. 17 and 18. To calculate the *IV* characteristics of the stack of the intrinsic JJ, we solve the system of nonlinear second-order differential equations (the one-dimensional CCJJ+DC model) for gauge-invariant phase differences $\varphi_l(t)$ between S layers l and $l+1$ in the presence of electromagnetic irradiation:

$$\begin{cases} \dfrac{\partial \varphi_l}{\partial t} = V_l - \alpha(V_{l+1} + V_{l-1} - 2V_l), \\ \dfrac{\partial V_l}{\partial t} = I + I_l^{\text{noise}} - \sin\varphi_l - \beta\dfrac{\partial \varphi_l}{\partial t} + A\sin(\omega t), \end{cases} \tag{1}$$

where t is the dimensionless time normalized to the inverse plasma frequency ω_p^{-1}, $\omega_p = \sqrt{2eI_c/\hbar C}$, C is the capacitance of the junctions, $\beta = 1/\sqrt{\beta_c}$, β_c is the McCumber parameter, α gives the coupling between junctions [4], and A is the amplitude of the radiation. A small noise is added to the bias current. The noise is produced by random number generator (white noise) and its amplitude 10^{-8} is normalized to the critical current value I_c [18].

In our simulations, Runge–Kutta methods of order 4(5) were used. We measure the voltage in units of $V_0 = \hbar\omega_p/(2e)$, the frequency in units of ω_p, the bias current I and the amplitude of radiation A in units of I_c. In this work numerical calculations have been done for a stack of 10 junctions with the coupling parameter $\alpha = 0.05$, dissipation parameter $\beta = 0.2$, and periodic boundary conditions. The periodic boundary conditions simulate a stack of infinite length and thus the exact number of junctions in our simulations is relatively unimportant. We use a conservative estimate for the value of $\alpha = 0.05$ in our simulations, merely in order to capture the principal features of the observed effects. Analysis of capacitive coupling parameter values in HTSC was presented in Ref. 19. Estimations for BSCCO place α in the interval [0.05–1]. Particularly, the value of $\alpha = 0.1$ was used in Ref. 20. This form of coupling between junctions, in the CCJJ+DC model, leads to a branch structure in the *IV* characteristics which is in qualitative agreement with currently available experimental measurements on intrinsic JJs [1,8]. We note that the qualitative results concerning the discussed topics are not very sensitive to changes in the parameter value over the interval $0.05 \le \alpha \le 1$. The details of the model and simulation procedure were presented in Refs. 17 and 18.

The electric charge density in the superconducting layer [18,21] is determined by the difference between the voltages V_l and V_{l+1} in the neighboring insulating layers, i.e.

$$Q_l = Q_0\alpha(V_{l+1} - V_l), \tag{2}$$

where $Q_0 = \varepsilon_r\varepsilon_0 V_0/r_D^2$, ε_r is the relative permittivity and ε_0 is the permittivity of free space. For brevity we will refer to Q simply as the charge. In the presented results we have normalized Q to Q_0. For $r_D = 3\cdot10^{-10}$ m, $\varepsilon_r = 25$, $\omega_p = 10^{12}\,\mathrm{s}^{-1}$, we get $V_0 = 3\cdot10^{-4}$ V and $Q_0 = 8\cdot10^5$ C/m^3. So, at $Q = Q_0$ for a superconducting layer with area $S = 1$ μm^2 and thickness $d_s = 3\cdot10^{-10}$ m the charge value is about $2.4\cdot10^{-16}$ C. This value of charge is sufficiently high to play a significant role in the physical processes in the stack of intrinsic Josephson junctions in high-temperature superconductors.

3. Analysis of subharmonic appearance with increase in radiation power

In this section we analyze the *IV* characteristics at two different amplitudes ($A = 0.17, 0.35$) and demonstrate general features of subharmonics appearance with increase in power of radiation. The total *IV* characteristic of the stack of coupled JJ is characterized by multiple branch structure related to the distribution of JJs among rotating and oscillating states [22,23]. Transition from the outermost branch to inner branches happens at parametric resonance, coinciding with the creation of a longitudinal plasma wave which effectively stabilizes the outer (all rotating) branch [13]. Influence of the external electromagnetic radiation leads to the appearance the SS and their subharmonics on the *IV* characteristic and additional parametric resonances in the system [14]. Below we concentrate on the features of the coupled JJs related to the current intervals of SS subharmonics on the outermost branch.

Figure 1(a) demonstrates a part of the *IV* characteristic together with the differential resistance dV/dI for a stack with 10 coupled JJ under radiation with frequency $\omega = 2.0$ and amplitude $A = 0.17$. The complete one-loop *IV* characteristic is shown in the inset. We see clearly the manifestation of the main SS at $V = 20$ and the subharmonics 2/3 at $V = 13.33$, 3/5 at $V = 12$, and 4/7 at $V = 11.42$. Calculation of the differential resistance dV/dI as a function of V identifies the additional subharmonics 5/8 and 3/4 which are not manifested clearly in *IV* characteristic.

The number of observable subharmonics generally increasing with an increase in the amplitude of radiation. This trend is demonstrated in Fig. 1(b), which presents the result of a simulation at $A = 0.35$. To analyze these results we use the algorithm of continued fractions (CF) developed in Ref. 24. It was noted there that, in general, the Shapiro and subharmonic steps follow the CF formula given by

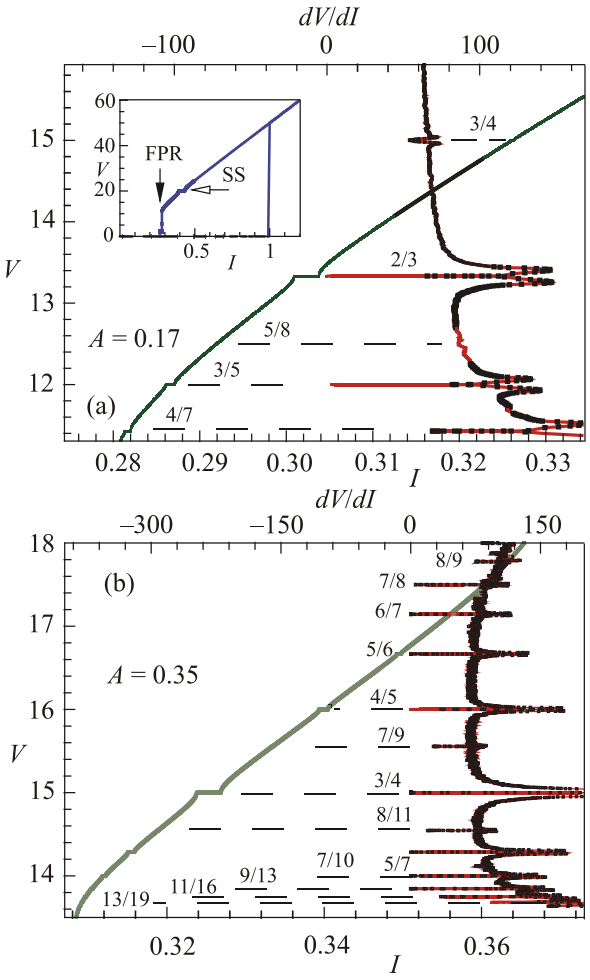

Fig. 1. (Color online) (a) Subharmonics in a part of *IV* characteristics (green curve) for a stack containing 10 coupled JJs under radiation at the frequency $\omega = 2$ and amplitude $A = 0.17$. The remaining two parameter values are $\alpha = 0.05$ and $\beta = 0.2$. The inset shows the complete *IV* characteristics of the same stack. Differential resistance dV/dI (red curve plotted on upper and left axes) is shown as a function of the average voltage V. (b) The same as in (a) for $A = 0.35$.

$$V = \left(N \pm \cfrac{1}{n \pm \cfrac{1}{m \pm \cfrac{1}{p \pm \ddots}}} \right) \omega, \tag{3}$$

where $N, n, m, p, \ldots$ are positive integers. Terms that only differ in N form a first-level sequence and describe Shapiro step harmonics. The other terms describe subharmonics. Those differing in N and n are called a second-level sequences; those differing in N, n and m, third-level sequences, etc. The order in appearance of the different CF depends on the parameters of JJ and external radiation [24]. The continued fraction in the form of Eq. (3) provides a very convenient way of mapping the potentially infinite

number of ratios p/q (with p and q positive integers that reflect the frequency-locking [6] $p\omega_J = q\omega$ between the Josephson and external radiation oscillations) to the observable hierarchical structure in the IV characteristic. Following Eq. (3), we can find that the subharmonics 2/3, 3/5 and 4/7 observed at $A = 0.17$ belonged to the third-level sequence, with $N = 1$ and $n = 2$, determined by the formula $1 - 1/(2 + 1/m)$. This sequence has a limiting value of 1/2, as m tends to infinity. Similarly the step 5/8 belongs to $1 - 1/(3 - 1/m)$. The step 3/4 belongs to a second order sequence given by

$$V = \left(N - \frac{1}{n} \right) \omega \qquad (4)$$

with $N = 1$.

A clear realization of two staircases is found at $A = 0.35$. The first one forms the continued fraction (4) which unites the observed steps 3/4, 4/5, 5/6, 6/7, ... This continued fraction starts at 0 and approaches 1. The steps 1/2 and 2/3 are out of the hysteresis region and that is why we do not observe them. The second continued fraction realized at $A = 0.35$ is $N - 1/(n + 1/m)$ with $N = 1$ and $n = 3$ which reflects an appearance of the steps 3/4, 5/7, 7/10, 9/13,..., as we can see in Fig. 1(b). Based on this classification we have analyzed the charging of S layers in the next section.

4. Charging of S layers

To visualize the subharmonic steps more clearly, and over a continuous range of the relevant parameter values, we have plotted, using the red color map in Fig. 2, the magnitude of the differential resistance as a function of the radiation amplitude and bias current. To see when charge develops on each of the step we have superimposed a plot of the magnitude of the maximum charge in the S layers $Q_{\max}$ on the same figure, using the blue color map. Regions of no charge, or charge in excess of 0.08 (as may occur for inner branches), have been rendered as being transparent, so as not to obscure the underlying plot. The V-shape that can be seen on the right hand side of the figure is the main SS harmonic, which has a linearly increasing width for small A. The expected Bessel behavior of the width dependence only manifests itself at much larger A. As we see, with increase in A the left side, just off the main SS, becomes "charged". On the other hand, the far left part of Fig. 2 is related to the branching region, i.e., it corresponds to inner branches. In this paper we concentrate on the SS subharmonics that occur on the outermost branch below first SS harmonic. Some of the subharmonic steps can be seen towards the middle of the figure.

In this view the steps show up as regions of zero resistance (which correspond to the reddish-brown region of the left color map). The subharmonics correspond to regions in the parameter space where the rotation number (or winding number) of the dynamical system is rational, forming, in mathematical terms, Arnold tongues [25]. The most prominent sequence of subharmonic steps that can easily be seen in the figure correspond to the locking ratios 2/3, 3/4, 4/5.... Interestingly, these steps follow the second level continued fraction sequence, given by Eq. (4), with $n = 3, 4, 5 \ldots$.

Another notable feature of Fig. 2 is the fact that all the subharmonic steps do not appear at once, for a given amplitude. This observation suggests that the onset of charging may in fact not be simply related to a change in one of the variables alone, but rather to some combination of variables.

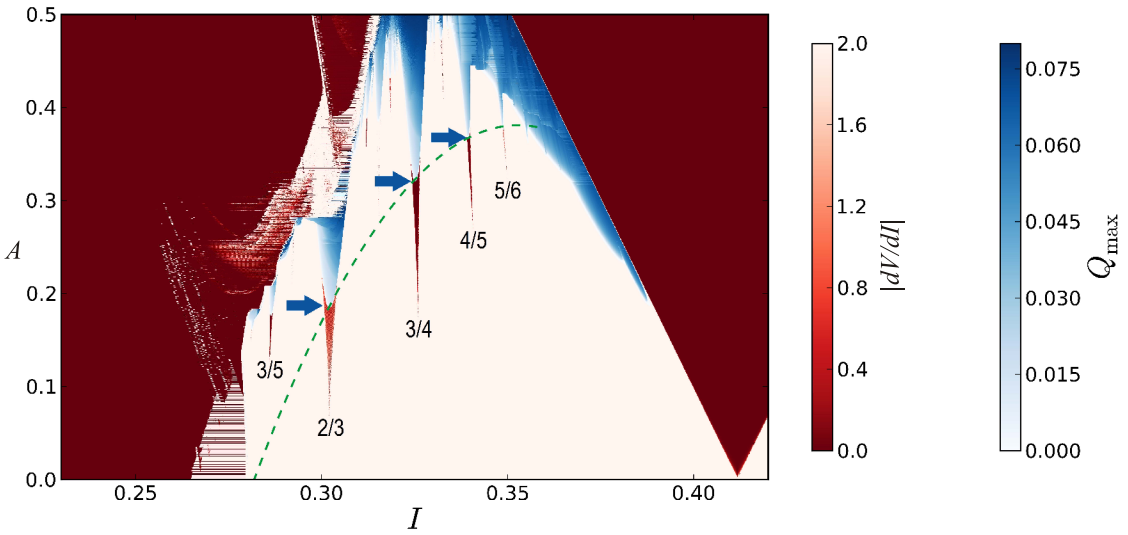

Fig. 2. (Color online) "Charging" of the Shapiro step subharmonics as a function of radiation amplitude and dc-bias current. Arrows indicate the points when the steps are becoming "charged". The green dashed line stresses the parabolic dependence of $A(I)$ along the transition boundary.

For example, to realize all the main subharmonics in an experiment, one could vary I and A simultaneously to measure the average voltage V on a curve that passes through all the visible steps. In principle, such a measurement is no more difficult to make than for the standard IV characteristic. Potential applications of the charging on any particular subharmonic can also be exploited by fixing the bias current on that subharmonic, and then varying the radiation amplitude above and below the thresholds for charging, that can be seen in Fig. 2.

The curve passing through the points on the figure where the subharmonics become "charged" (marked by the blue arrows) can be fitted very accurately by a parabolic dependence of A on I. This dependence is shown by the (green) dashed curve in the figure. So, we arrive at the possibility of a novel experiment for studying parametric instabilities and charging of S layers, based on the simultaneous variation of the bias current and radiation amplitude. When we measure the average voltage at each value $I(A)$, we get an IV characteristic, on which each point corresponds to a different value of A. At the same time, such an $I(A)$ V characteristic would manifest all of the most prominent subharmonics in one sweep. By shifting the $I(A)$ curve to above the critical curve for the onset of charging (see Fig. 2), the charge on all the principal subharmonics could be changed simultaneously.

Let us now demonstrate that the results presented in Fig. 2 are in agreement with traditional study of IV characteristics and charging of S layers at fixed value of radiation amplitude. We concentrate on an appearance of the electric charge in S layers in current intervals related to the SS subharmonics. It is known that in the case of a single JJ the external radiation leads to a decrease of the hysteresis region in IV characteristic with an increase in the radiation amplitude A, i.e., it leads to the decrease of the critical current and the increase of the return current I_R [4]. For a stack of coupled JJs the external radiation leads additionally to a series of novel effects related to the parametric resonances and the LPWs propagating along the c axis [4,26]. Some preliminary results concerning an appearance of charge in the S layers of the stacked JJ in the current interval corresponding to the SS harmonics [14] and subharmonics [27,28] were presented earlier. We show here that "charging of subharmonics" have specific new features.

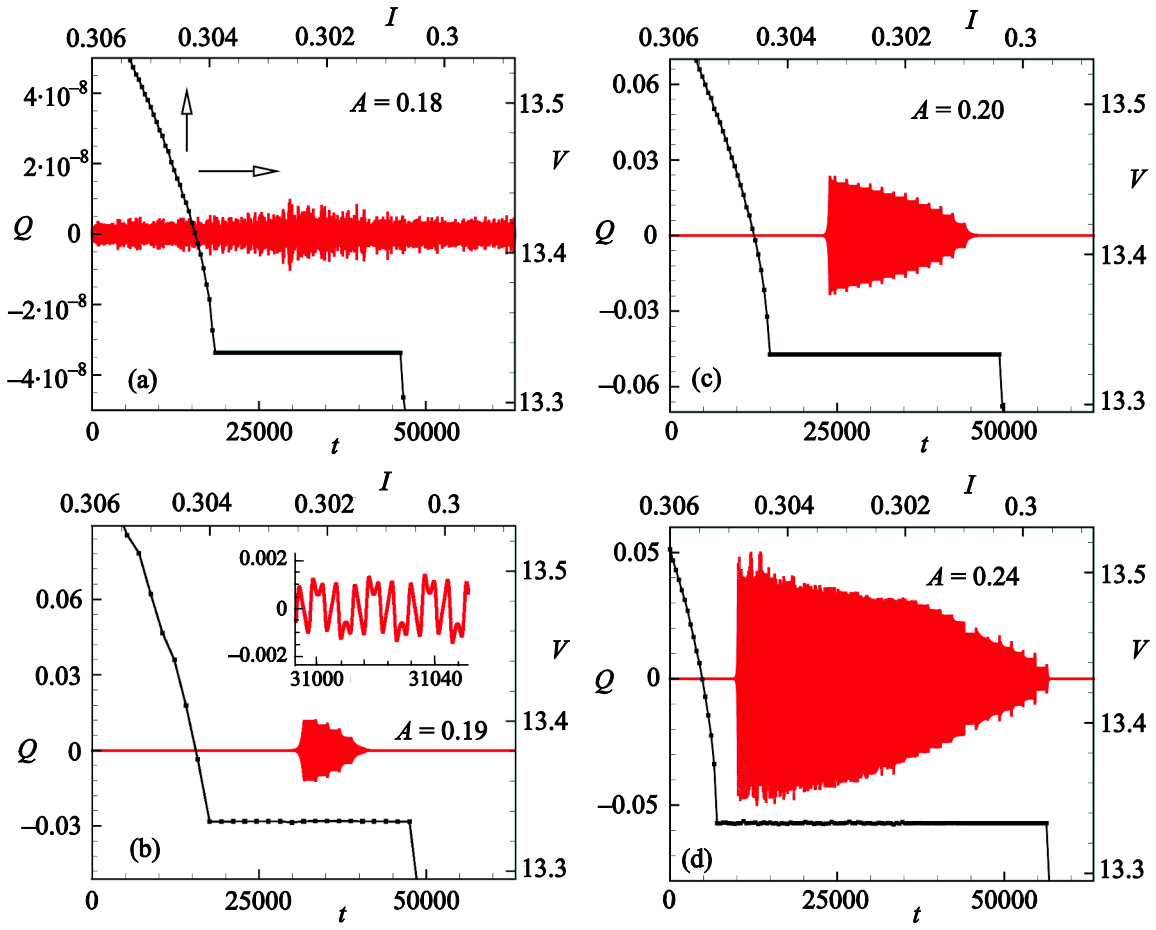

Fig. 3. (Color online) Demonstration of charge oscillation growth in S layers with increase in A over the current interval corresponding to the steps 2/3. The figures present charge-time dependence characterized by left and lower axes, and IV characteristic characterized by right and upper axes (black curves). The value of A is indicated in each figure. Inset to (b) shows an enlarged view of the charge oscillations.

Figure 3 demonstrates the appearance and growth of charge in the first superconducting layer of the stack with an increase in the amplitude of radiation, within a current interval corresponding to the subharmonic step 2/3. In the other layers the development of charge takes place similarly. Here we show the charge-time dependence together with the *IV* characteristics at frequency $\omega = 2$ and four different values of radiation amplitude. The charge oscillations are not actually manifested until the amplitude exceeds $A = 0.18$. Before this value the charge is at noise level (see Fig. 3(a)). We can see that this result is in agreement with the corresponding region in Fig. 2. The oscillations start growing around the center of the subharmonic step current interval and expand along the step with an increase in amplitude. This development continues until a transition of the JJs to the chaotic state and the consequent fragmentation of the step. At $A = 0.19$ the charge value becomes larger (see Fig. 3(b)): $Q \simeq 0.01$. Actually, the growing of charge is related to the parametric resonance in the coupled system of JJs. Inset shows the character of charge oscillations at the beginning of the parametric resonance corresponding to the bias current $I = 0.3026$. With increase in A the value of charge grows (see Fig. 3(c)) and it eventually occupies the total current interval corresponding to the SS subharmonic. We see this in Fig. 3(d), which is for $A = 0.24$. As follows from Fig. 2, the step 2/3 demonstrates anomalous behavior at amplitude larger $A = 0.27$. This behavior is also related to the appearance of chaos in system of junctions with increase in A and fragmentation of the step [28]. As can be seen in Fig. 2, there is a regular increase of the step widths and "charging" for 3/4, 4/5, and 5/6. The "charging" of the last two steps overlaps with a charge appearing near the left side of the main SS.

5. Cascade of subharmonic parametric resonances

As it was noted [13,21], the coupled system of JJs without external radiation has a longitudinal plasma wave as a eigenmode of the system. The eigenmode is excited at parametric resonance. The resonance is manifested in the *IV* characteristics as a breakpoint before transition from the outermost to the inner branch. With external electromagnetic radiation an additional radiation related parametric resonance appears around the Shapiro steps [14]. Below we demonstrate the occurrence of the parametric instabilities within the current intervals corresponding to Shapiro step subharmonics. In Fig. 4(a) the time series of the charge in the first superconducting layer of the stack is shown at the onset of the parametric instability for the subharmonic 2/3. We observe an exponential increase of the charge in time. To "prove" it, Fig. 4(b) shows the same time series on a logarithmic scale, demonstrating the expected linear dependence that characterizes parametric resonance, which was discussed in Ref. 14. Distribution of charge in S layers along the stack is presented in Fig. 4(c).

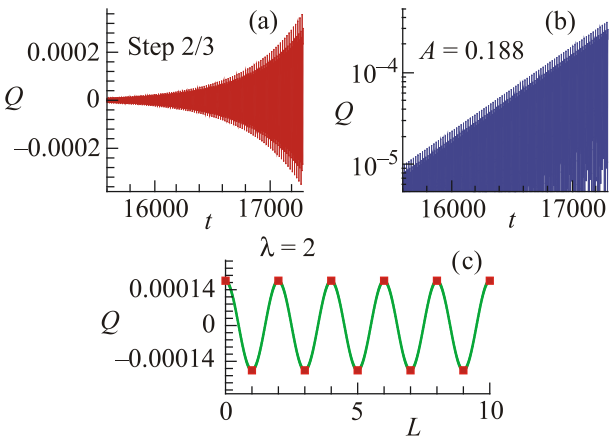

Fig. 4. (Color online) Demonstration of the parametric instability for the subharmonic step 2/3. (a) Time series of charge in first layer; (b) The same on logarithmic scale; (c). The corresponding longitudinal plasma wave of wavelength $\lambda = 2$.

In this case we observe the creation of a longitudinal plasma wave of wavelength $\lambda = 2$, where λ has been normalized to the lattice period.

Additional evidence for the parametric character of instabilities around the subharmonics follows from Fig. 5, where we compare the results of FFT analysis of voltage (in case of step without charging S layers) and charge oscillations. The FFT for voltage (Fig. 5(a)) shows the minimal frequency peak corresponding to the resonance condition for 2/3 subharmonic $f_J/2 = f_R/3$ with Josephson frequency and radiation frequency $f_R = f_J = 0.21201$. As we can see, $\omega_R = 2\pi f_R \approx 2$ coincides with applied radiation frequency. The other frequencies are "harmonics" for this SS subharmonic 2/3. Figure 5(b) gives the FFT spectrum of the charge oscillations. We see the minimal peak at double smaller frequency $f_{LPW} = f_J/4 = f_R/6$. This fact corresponds to the case of parametric resonance, as described in Ref. 21: the longitudinal plasma frequency is twice smaller then the smallest frequency presented in the voltage FFT analysis, and this demonstrates the well-known signature of parametric resonance.

To stress the common features of parametric instabilities for SS subharmonics, we show below the case for subharmonic step 3/4. The electric charge and *IV* characteristic is presented in Fig. 6(a). We see analogous "charging" of the S layers, as was seen previously for the step 2/3, when the current is within an interval corresponding to the step 3/4. Results of the FFT analysis of the voltage time series in the first JJ of the stack are shown in Fig. 6(b). Here we see that the lowest frequency corresponds to the subharmonic for which $f_J/3 = f_R/4$. The FFT analysis of the charge oscillations shows the appearance of a frequency $f_J/6$, which is half of the lowest frequency for the uncharged state.

The absence of the Josephson frequency in FFT spectrum demonstrates the fact that, at the chosen bias current

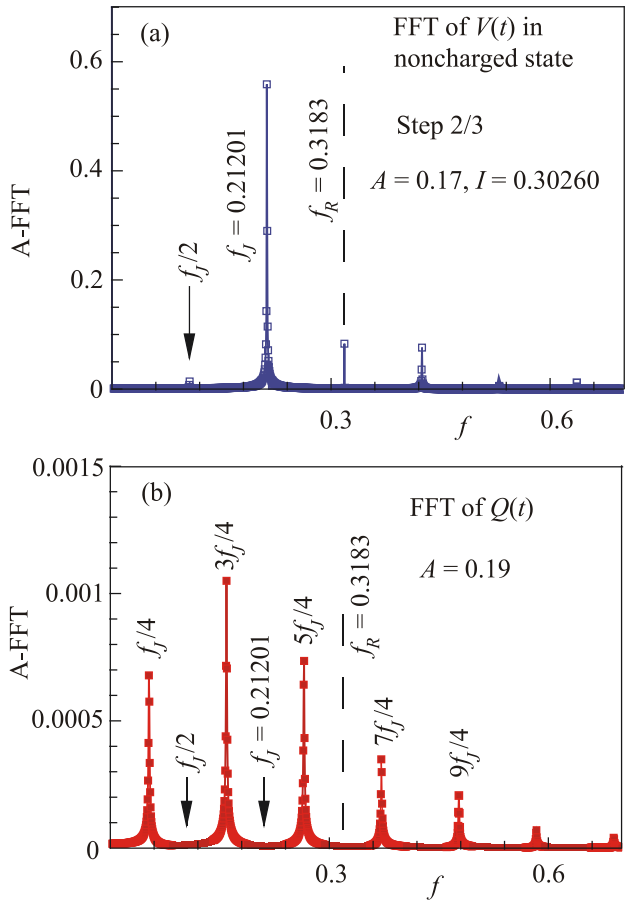

Fig. 5. (Color online) (a) Results of FFT analysis of voltage oscillations at a current within the interval corresponding to the step 2/3, for the "noncharged state" at the radiation amplitude A = = 0.17; (b) The same FFT analysis for the charge oscillations on the step 2/3 at $A = 0.19$.

the resonance condition $\omega_J = 2\omega_{LPW}$ is exactly fulfilled and the double period oscillation does not manifest itself. Really, the $Q(t)$ dependence was recorded at a bias current when the charge was exponentially growing, i.e., exactly at the resonance condition.

We have also investigated parametric instabilities around other steps (data are not presented here) and obtained the same features as described for the resonances associated with the steps 2/3 and 3/4. Differences might appear in value of the wavelength of the created LPW; particularly, it was found to be $\lambda = 5$, for the subharmonic 4/7.

6. Summary

We performed a precise numerical study of the phase dynamics of intrinsic JJs in high-temperature superconductors under applied electromagnetic radiation. We observed charging of the superconducting layers in the bias current interval corresponding to Shapiro step subharmonics. Formation of longitudinal plasma waves due to "charging" of SS subharmonics is demonstrated.

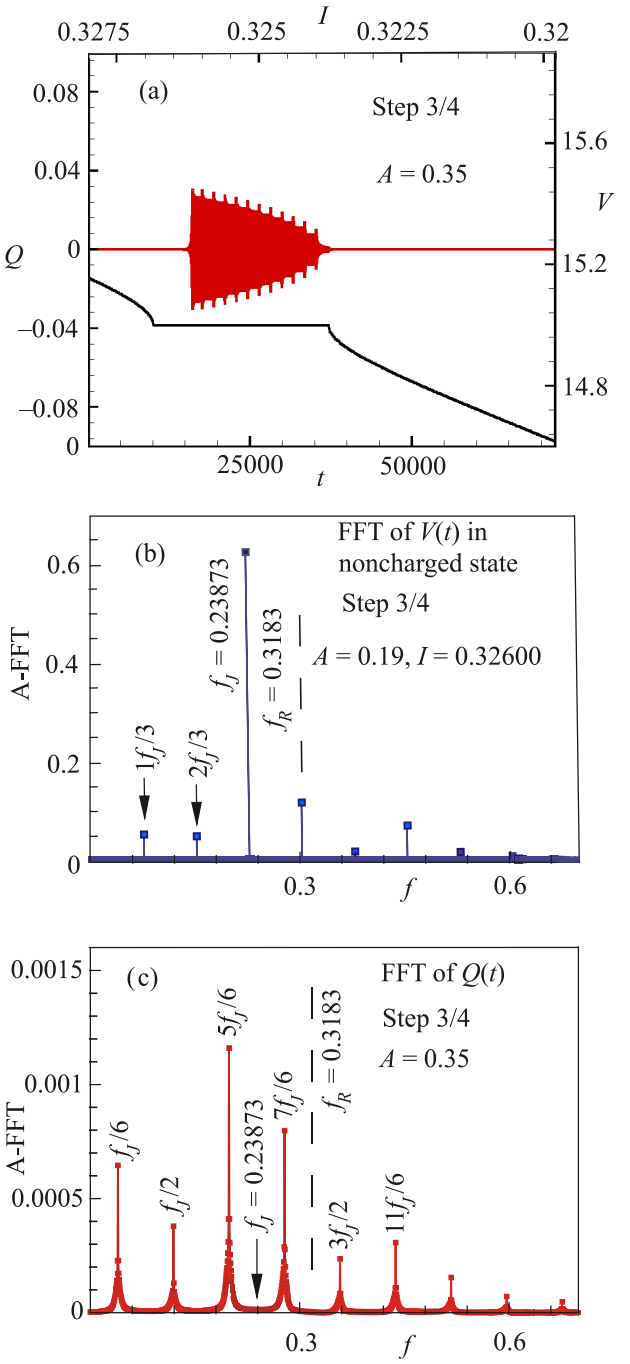

Fig. 6. (Color online) (a) Demonstration of electric charge in S layers in current interval corresponding to the SS subharmonics 3/4 together with IV characteristic (solid line, upper and right axes); (b) Results of FFT analysis of the voltage oscillations in the first JJ of the stack in noncharged state at $A = 0.19$ at current interval around $I = 0.32600$; (c) The same for charge oscillations in the first S layer at amplitude of radiation $A = 0.35$.

An essential feature, which may be important for future applications, is the difference between the parametric instabilities in case of subharmonics in comparison to those of Shapiro step harmonics. In the first case a much lower amplitude of radiation is required for the creation of the longitudinal plasma wave along the stack of junctions. This fact

may provide an unique possibility to create and control the excitation of the longitudinal plasma wave in layered superconductors. Longitudinal plasma waves in the system of junctions is a new element in comparison to the properties of the single Josephson junction. Its existence in layered superconductors was demonstrated experimentally (see, for example, Ref. 19) and it might play an essential role in certain physical phenomena that occur in high-temperature superconductors; particularly, in synchronization of Josephson oscillations in different junctions of the stack [30]. It also has bearing on chaos synchronization, which may find applications in secure communication [31].

There is a remarkable ordering in the sequence of realizable subharmonic steps: the most prominent steps correspond to lower order continued fraction sequences. It is therefore natural to ask whether the wavelengths of the excited longitudinal plasma wave, associated with the charge on each subharmonic, may also follow a relatively simple rule, like the well known case of standing waves on a string. In the present case, however, the situation is somewhat more complicated, firstly due to the discrete nature of the system (the charge is only know at each junction) and secondly due to the an-harmonic nature of the charge waves. Thirdly, since the charge on the layers appears according to the strength of the nonlinear coupling between the junctions, the effect of coupling should be taken carefully into account. Finally, in trying to establish a rule for predicting the wavelength, one also has to bear in mind the physical significance attached to changes in each of the system parameters. For example, the coupling strength α is related to the overall length of the stack, and even changes in the bias current may effect the dispersion relation for the system. Thus, to answer this very interesting question conclusively would require more extensive exploration of the parameter space for different numbers of junctions, different coupling strengths, damping, radiation frequencies, etc.

Acknowledgments

Yu.M.S. and I.R.R. thank M.R. Kolahchi, V.P. Koshelets, G.A. Ovsyannikov, M.Yu. Kupriyanov, V.M. Pudalov, L.A. Falkovsky for detailed discussion of some results of this paper and D.V. Kamanin, M.L. Lekala for their support under the JINR SA agreement. This work is based on the research supported by the National Research Foundation of South Africa and partially by the RFBR research projects 15-51-61011 and 12-29-01207.

1. U. Welp, K. Kadowaki, and R. Kleiner, *Nature Photonics* **7**, 702 (2013).
2. B.D. Josephson, *Adv. Phys*. **14**, 419 (1965).
3. P.W. Anderson and A.H. Dayem, *Phys. Rev. Lett*. **13**, 195 (1964).
4. T. Koyama and M. Tachiki, *Phys. Rev. B* **54**, 16183 (1996).
5. W. Buckel and R. Kleiner, *Superconductivity: Fundamentals and Applications*, Wiley-VCH, Verlag GmbH Co. KGaA (2004).
6. K.K. Likharev, *Dynamics of Josephson Junctions and Circuits*, Gordon and Breach, Philadelphia (1986).
7. C.A. Hamilton, *Rev. Sci. Instrum*. **71**, 3611 (2000).
8. A.A. Yurgens, *Supercond. Sci. Technol*. **13**, R85 (2000).
9. H. Wang, J. Chen, P. Wu, T. Yamashita, D. Vasyukov, and P. Muller, *Supercond. Sci. Technol*. **16**, 1375 (2003).
10. Yu.M. Shukrinov and P. Seidel, *Elektronika* **6**, 52 (2011).
11. H.B. Wang, P.H. Wu, and T. Yamashita, *Phys. Rev. Lett*. **87**, 107002 (2001).
12. D.A. Ryndyk, *Phys. Rev. Lett*. **80**, 3376 (1998).
13. Yu.M. Shukrinov and F. Mahfouzi, *Phys. Rev. Lett*. **98**, 157001 (2007).
14. Yu.M. Shukrinov, I.R. Rahmonov, and M.A. Gaafar, *Phys. Rev. B* **86**, 184502 (2012).
15. V.N. Belykh, N.F. Pedersen, and O.H. Soerensen, *Phys. Rev. B* **16**, 4860 (1977).
16. S.-Z. Lin and A. E. Koshelev, *Physica C* **491**, 24 (2013).
17. Yu.M. Shukrinov, F. Mahfouzi, and P. Seidel, *Physica C* **449**, 62 (2006).
18. Yu.M. Shukrinov and M.A. Gaafar, *Phys. Rev. B* **84**, 094514 (2011).
19. M. Machida and T. Koyama, *Phys. Rev. B* **70**, 024523 (2004).
20. M. Machida, T. Koyama, and M. Tachiki, *Phys. Rev. Lett*. **83**, 4618 (1999).
21. Yu.M. Shukrinov, F. Mahfouzi, and M. Suzuki, *Phys. Rev. B* **78**, 134521 (2008).
22. R. Kleiner, F. Steinmeyer, G. Kunkel, and P. Muller, *Phys. Rev. Lett*. **68**, 2394 (1992).
23. Yu.M. Shukrinov, F. Mahfouzi, and N. Pedersen, *Phys. Rev. B* **75**, 104508 (2007).
24. Yu.M. Shukrinov, S.Yu. Medvedeva, A.E. Botha, M.R. Kolahchi, and A. Irie, *Phys. Rev. B* **88**, 214515 (2013).
25. R.C. Hilborn, *Chaos and Nonlinear Dynamics: An Introduction*, Oxford University Press, New York (2000), 2nd.
26. R. Kleiner, T. Gaber, and G. Hechtfischer, *Phys. Rev. B* **62**, 4086 (2000).
27. H. Azemtsa-Donfack, Yu.M. Shukrinov and I.R. Rahmonov, *Proc. SAIP2014, the 59th Ann. Conf. of the South African Institute of Physics*, C. Engelbrecht and S. Karataglidis (eds.), **59**, 24 (2014).
28. Yu.M. Shukrinov, H. Azemtsa-Donfack, and A.E. Botha, *JETP Lett*. **101**, 251 (2015).
29. Y. Matsuda, M.B. Gaifullin, K. Kumagai, K. Kadowaki, and T. Mochiku, *Phys. Rev. Lett*. **75**, 4512 (1995).
30. S.-Z. Lin, X. Hu, and L. Bulaevskii, *Phys. Rev. B* **84**, 104501 (2011).
31. A.E. Botha, Yu.M. Shukrinov, S.Yu. Medvedeva, and M.R. Kolahchi, *J. Supercond. Novel Magnetism* **28**, 349 (2015).